



Journal of Mining and Earth Sciences

Website: <http://jmes.humg.edu.vn>



3D inversion of 2D electrical resistivity data for geotechnical analysis

Dat Ngoc Pham^{1,*}, Kien Ngoc Pham², Phong Hop Lai¹, Ninh Thi Duong¹, Trang Hong Pham¹, Tuan Dang Tran¹

¹ Vietnam Academy of Science and Technology, Hanoi, Vietnam

² Hanoi University of Mining and Geology, Hanoi, Vietnam



ARTICLE INFO

Article history:

Received 07th May 2022

Revised 24th Aug. 2022

Accepted 13th Sept. 2022

Keywords:

3-dimension,
Electrical resistivity,
Geotechnical analysis,
Inversion,
Resistivity,
Tomography.

ABSTRACT

Geophysical methods are effective tools for geotechnical analysis. In particular, the two-dimensional electrical resistivity method is widely applied in the determination of broken, cracked, and karst cave structures in many countries around the world. The information given by this method plays an important role in preventing and mitigating the risk of geological hazards caused by geological structures. Geotechnical analysis is also an important step in civil construction. However, the interpretation of two-dimensional problems with individual sections still has certain limitations, such as the delineation of the spatial distribution of interesting objects in the entire survey area. We propose a new data processing procedure for the two-dimensional electrical resistivity methods based on rearranging the data as the input of three-dimensional inversion. If the distribution of survey lines is dense enough, we can use two-dimensional data to solve the three-dimensional inverse problems. This inversion will give us a diagram of resistivity distribution in three-dimensional space, which is intuitive and high detail in identifying interesting objects. In this study, the authors have solved the three-dimensional inverse problems from the two-dimensional electrical resistivity survey carried out in the Hoa Lac area, west of Hanoi city. The result shows that the resistivity distribution in three-dimensional space not only increases the intuition but also the accuracy in reflecting the spatial distribution of hidden underground objects. This also defines the localization and determination of fracture zones in the study area as more reliable than explained in each section according to the results of solving two-dimensional inverse problems. The effectiveness of this new method has been proven when compared with drilling results in the studied area.

Copyright © 2022 Hanoi University of Mining and Geology. All rights reserved.

*Corresponding author

E - mail: ngocdatdvlk52@gmail.com

DOI: 10.46326/JMES.2022.63(6).06

1. Introduction

Ground crack and land subsidence occur ubiquitously over the world. They are the geological hazards caused by natural and geological conditions and human activities. These hazards adversely affect people's lives and cause huge damage to many regions in Vietnam. For example, the Karst subsidences at Tan Hiep (Quang Tri province) in 2006; at Ham Yen and Yen Son (Tuyen Quang province) in 2007; at Mai Chau, Kim Boi (Hoa Binh province) in 2010. The land subsidence not only destroyed buildings and civil constructions but also led to the loss of freshwater supply. Thus, the study on positioning and determining the cause of these hazards is critically important to mitigate their risks in dangerous regions.

Two-dimensional (2D) electrical resistivity tomography (ERT) method is widely used to investigate the caves and fracture zones in the subsurface. For instance, Szalai et al. (2014) and Duszyński et al. (2017) combine this method with other investigations to evaluate the structure and the link of the system of fractures and caves in the southwest region of Poland. In Vietnam, this method is also used to identify and forecast the risky regions related to ground crack and land subsidence (Doan and Vu, 2008; Le, 2012; Pham et al., 2018).

In recent years, the three-dimensional (3D) ERT is becoming an effective tool for near-surface geophysical investigation. For example, it is applied for the monitoring of the movement of water through a vadose zone in Park (1998). Weller et al. (2000) and Ogilvy et al. (2002) investigate the waste deposit region using this method. Also, Represas et al. (2005) applied this method in mining investigation. The applications in archeology and vacant buildings are proposed in Sultan et al. (2006) and Soupios et al. (2007). Sultan and Monteiro Santos (2008) combine the 1D and 3D ERT methods to distinguish the clay formations from the sand layers in the geotechnical investigation. In Vietnam, the application of 3D ERT for geotechnical analysis in civil construction is still rare.

The 3D ERT is more accurate than the 2D method for figuring out 3D objects in the subsurface. The 2D method gives the cross-

section in a single tomography profile. The distribution of the objects is then correlated between the cross-sections in the study area. This correlation may lead to an inaccurate interpretation of 2D resistivity data. Meanwhile, the inversion of the 3D data generates a distribution of electrical resistivity in the volume of investigation such that the position of the objects is better determined.

In this paper, we introduce our application of 3D inversion of 2D ERT data set for geotechnical analysis at a civil construction in Hoa Lac (Hanoi, Vietnam). The result of the 3D is then compared to those of the 1D and 2D. The risky objects related to caves and fractures in the subsurface are better determined by the volumes of low resistivity in the 3D resistivity image. Thus, the 3D inversion of resistivity data is proposed to be used in other regions when detailed data is obtained.

2. Materials and methods

2.1. Study area and geological settings

The study area is a civil construction located in a high-technology zone in Hoa Lac (western-north of Ha Noi). It is 460 m in length in the x-direction and 200 m in the y-direction (Figure 1). This area is at the margin of the Red River trough, including a basement and an overlying sedimentary. The basement consists of eruption rocks of Vien Nam (T_{1vn}) and Tan Lac ($T_{1o\ t}$) formations, and carbonate rocks of Dong Giao formation ($T_{2a\ dg}$). This basement is broken by many faults, creating weak subsidence in the Cenozoic era. The sedimentary is mainly formed by Quaternary rocks of Vinh Phuc and Thai Binh formations, which have a thickness from 38÷65 m (Bui, 2012).

The fractured zones and caves in the area contain water and have a lower resistivity compared to the surrounding rocks. This resistivity property allows us to apply 3D ERT for figuring out the distribution of the risky volume that relates to fractured zones and caves.

In the study area, 210 resistivity sounding measurements have been carried out within 6 profiles elongated in the x-direction (Figure 2). The receiver spacing in each profile is between 15 and 20 m, and the spacing between two adjacent profiles is 50 m in the y-direction.

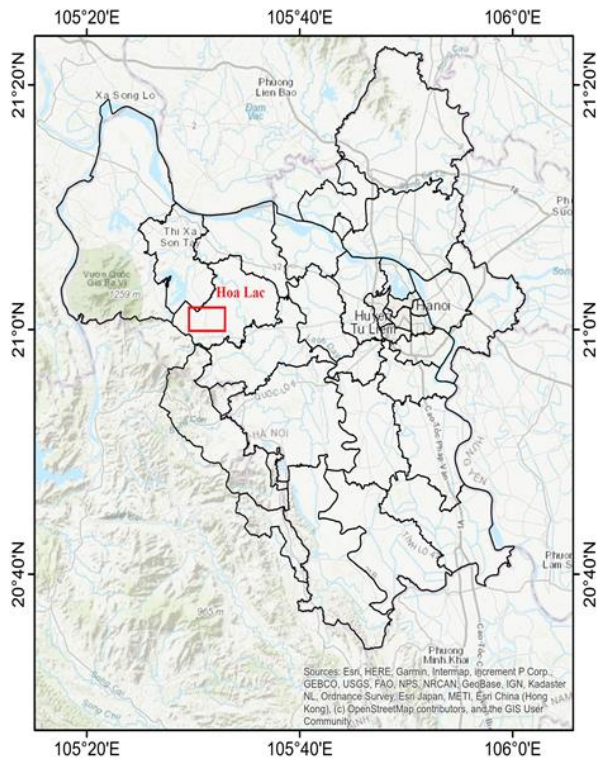


Figure 1. The study area.

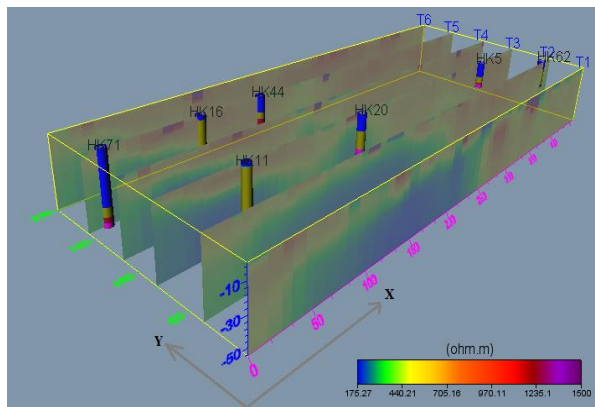


Figure 2. The 2D electrical resistivity tomography profiles.

Seven geological holes have been drilled in the area, on the profiles (T2, T3, and T5 in Figure 2). The borehole analysis is used to validate the ability of resistivity sounding to determine the region of possible ground cracks and land subsidence.

2.2. Algorithm and data observation

There are numerous algorithms for 3D inversion of electrical resistivity data. The most widely used technique is the finite difference

method (FD). This method is proposed in several research including Zhang et al. (1995), Zhao and Yedlin (1996), Loke and Barker (1996), and Spitzer (1998). Other techniques for solving 3D electrical resistivity problems are the finite element (FE) method (Yi et al., 2001) and the finite volume (FV) method (Pidlisecky et al., 2007).

The computation cost for 3D inversion is thoroughly considered in Loke and Barker (1996). The authors propose a technique that reduces two-thirds of the maximum data measures without a significant decrease in the resolution of 3D inversion results. Also, the starting model is a homogeneous half-space, which helps to reduce the computing time. These advantages are further studied in Loke (2010) for geoelectrical imaging.

Although the finite element method has its advantage over the finite difference method in dealing with the tomography, we apply the FD method in this study because of the negligible change in elevation of the area. Thus, the method of Loke (2010) is utilized.

We used the program RES3DINV of Loke (2010) for the inversion of 3D ERT data. In this program, there are four accepted types of data sets. The first type is an ideal 3D configuration, where the electrodes are located in either square or rectangular mesh, with the measurement carried out in an arbitrary direction. The second type obtains the data in both x- and y-direction, but measures only a few data at the corner of the mesh. The third type is the second without the measurement at the mesh corner. The last data set contains a series of parallel profiles in either x- or y-direction. This data set is the same as that of several 2D measurements, where the profiles are parallel to each other. With the fourth data set, the 2D inversion is carried out; the 3D inversion is then used for the combined data of all profiles in the investigating region.

At a single measuring point, the vertical electrical soundings are obtained. The apparent resistivity data at each point is then used for 1D inversion, grouped in a profile for 2D inversion. The 3D inversion is implemented with all resistivity data measured in the area. With this data set, the fourth type of data set in the RES3DINV program is adopted.

2.3. 3D inversion of electrical resistivity data

The 3D inversion is to find a resistivity model in three-dimensional volume based on minimizing the difference between measuring and computing data, where the latter is evaluated by solving the 3D forward problem. This work can be done by the smoothness-constrained least-squares method (Loke, 2010):

$$(J^T J + \lambda F) \Delta q_k = J^T g + \lambda F q_k \quad (1)$$

where

$$F = \alpha_x C_x^T C_x + \alpha_y C_y^T C_y + \alpha_z C_z^T C_z \quad (2)$$

in which: C_x , C_y , and C_z are the roughness filters in x-, y-, and z-directions, respectively; J and J^T are the Jacobian matrix of partial derivatives and its transpose; λ is the damping factor; q is the model perturbation vector; g is the data misfit vector; k is the iteration number.

Because the starting model is homogeneous, the Jacobian can be computed analytically. The iteration ends when the misfit between computing and measuring data is less than a predefined small value. The method often converges after four or five iterations.

The computing model is discretized into a structured grid consisting of rectangular prisms. The size of the prisms is extended from the top to the base of the model (Figure 3). The electrodes are located at the nodes of the uppermost plane of the model. The resistivities of the prisms change in each iteration until convergence is reached. In this study, we applied the misfit between the forward computation and the observed data of 6 percent. It is a few percent higher than that for 3D resistivity measurement (2÷3 percent) because our data is collected from the 2D resistivity tomography.

In practice, the data is observed on the surface. Thanks to the FD method the electrode spacing and the distance between two adjacent profiles do not need to be the same. We collected data from all profiles to produce an input file for 3D inversion. Because the electrodes are located at the nodes of the 3D grid, the algorithm allows us to perform the inversion schedule.

Because the electrode spacing was 15÷20 m and the distance between profiles was 50 m, we chose the grid spacing of 2.5 m in both x- and y-

directions. This grid ensures all electrodes are located at the nodes on the surface. Thus, the horizontal resolution of 2.5 m can be resolved. Furthermore, the first layer of the 3D grid has a thickness of 1 meter, whereas the deeper layer has a larger thickness (Figure 3). These thicknesses are sufficient to resolve the thin weathering layer and the thicker bedrock in the study area.

3. Results

The 3D inversion result is shown in Figure 4. This result gives a general distribution in three-dimensional of the resistivity of the subsurface. In Figure 4, the uppermost layer has resistivity from

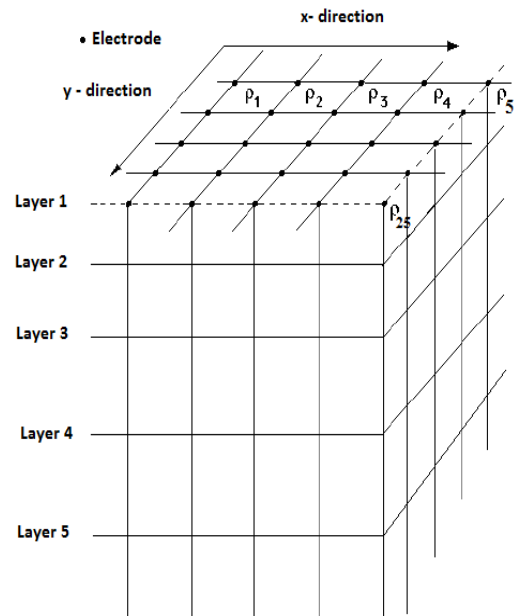


Figure 3. The structured grid for the 3D model (modified from Loke and Baker, 1996).

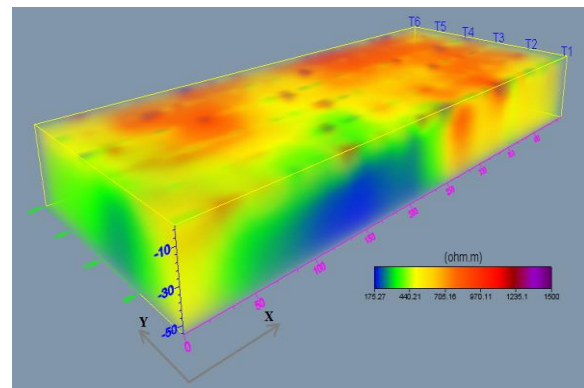


Figure 4. The 3D inversion results in the study area.

500÷700 Ohm.m with local distinctions between weathering soil and filling rocks. The lower layer whose resistivity is lower (about 200 Ohm.m) is related to the clay. In this layer, there are some positions where the resistivity is high (1000 Ohm.m). These positions may be the hard rocks.

To get detailed information on resistivity versus depth, 11 plane sections of 3D inversion are presented in Figure 5. These sections show the 3D results from the surface to the depth of 50 m. From the surface to the depth of 6 m, the local distinctions in resistivity appear. The resistivity values on the profiles T1, T2, and T3 are smaller than those on the profiles T4, T5, and T6. From 6÷30 m, the range of resistivity is wider than the upper plane sections. The low resistivity anomaly is mainly located in the western south of the study area. This anomaly region is clearly shown in the 30 m plane section. In the sections with a depth from 30÷60 m, the variation of resistivity is less than in the upper parts. The region of low resistivity (200÷300 Ohm.m) is in the left part of the panels (from 0÷240 m in the x-direction). In contrast, the region of high resistivity (larger than 300 Ohm.m) is in the right part.

In this study, we are interested in determining the position of the fractured zones and caves in the subsurface. According to the

previous geological and geophysical study, they are related to the region of low resistivity which is smaller than 250 Ohm.m (Bui, 2012; Pham et al., 2018). Figure 6 represents the low resistivity anomaly derived from the 3D inversion results. The distribution of the anomaly is intuitive. It is at the west of the study area and located below 20 m from the surface. In x-direction, the anomaly locates from 65÷245 m in the T1 profile, from 50÷230 m in the T2 profile, from 0÷220 m in the T3 profile, from 0÷120 m in the T4 profile, from 5÷100 m in T5 profile, and from 10÷50 m in T6 profile.

4. Discussion

The 3D inversion result provides a better spatial distribution of the resistivity as opposed to that of 1D and 2D inversions. The 1D result only gives the distribution versus depth (z-direction), whereas the 2D is the distribution in a cross section (i.e., x- and z-directions) (Figure 7).

Therefore, it is difficult to evaluate the location and volume of the fractured zones and caves in the study area with either 1D or 2D results. In this study, The 3D ERT method that helps to link the sounding data among the measuring profiles clearly shows the distribution of the low resistivity anomaly, which provides more information for geotechnical analysis.

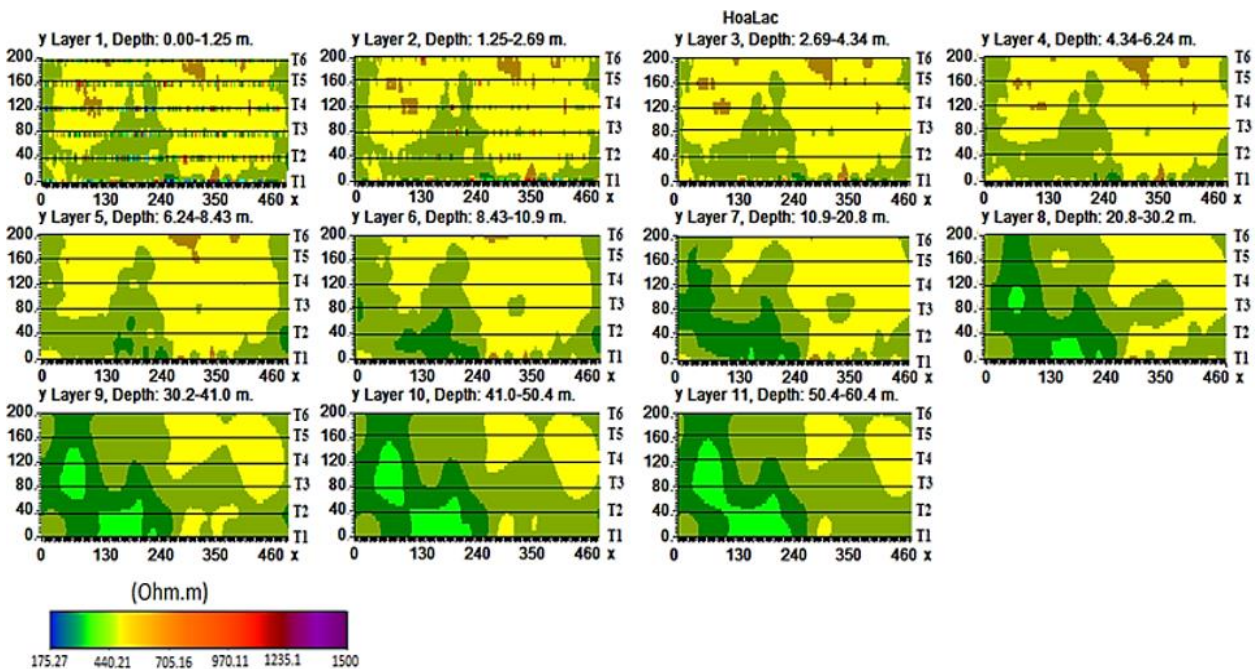


Figure 5. The plane sections of 3D resistivity inversion.

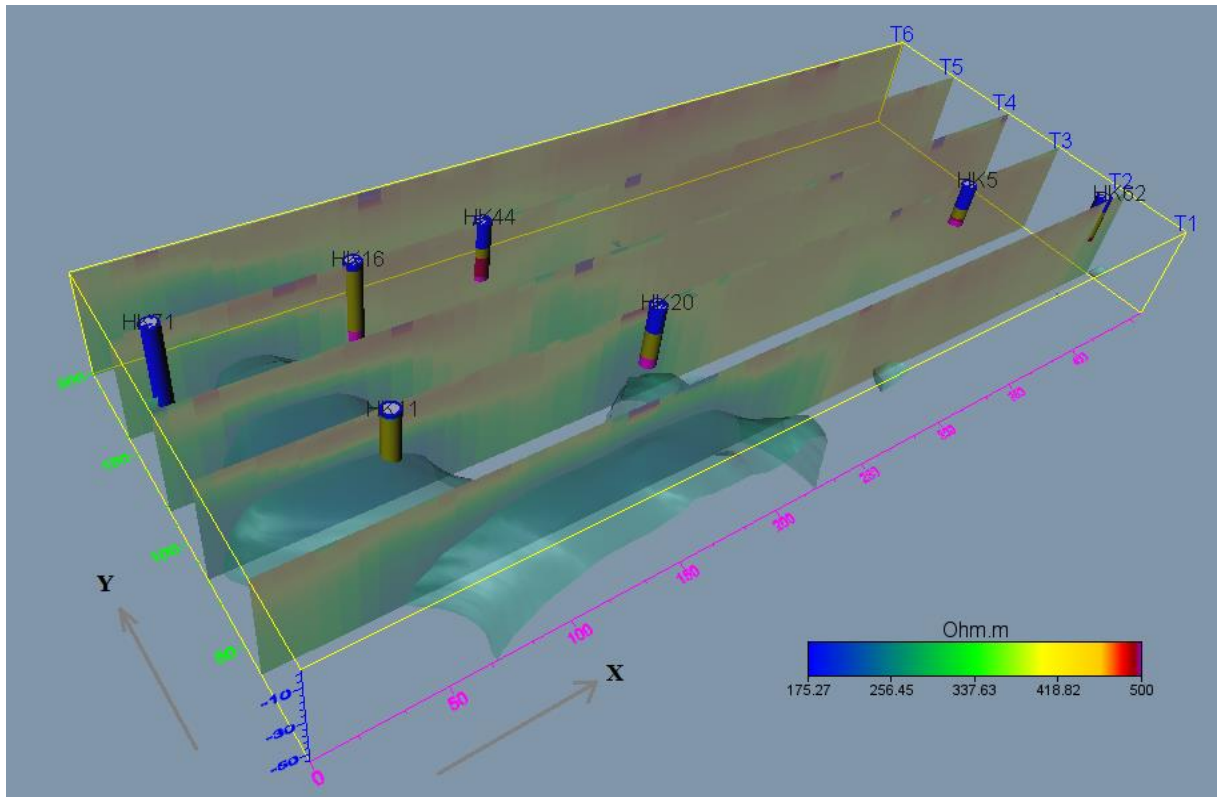
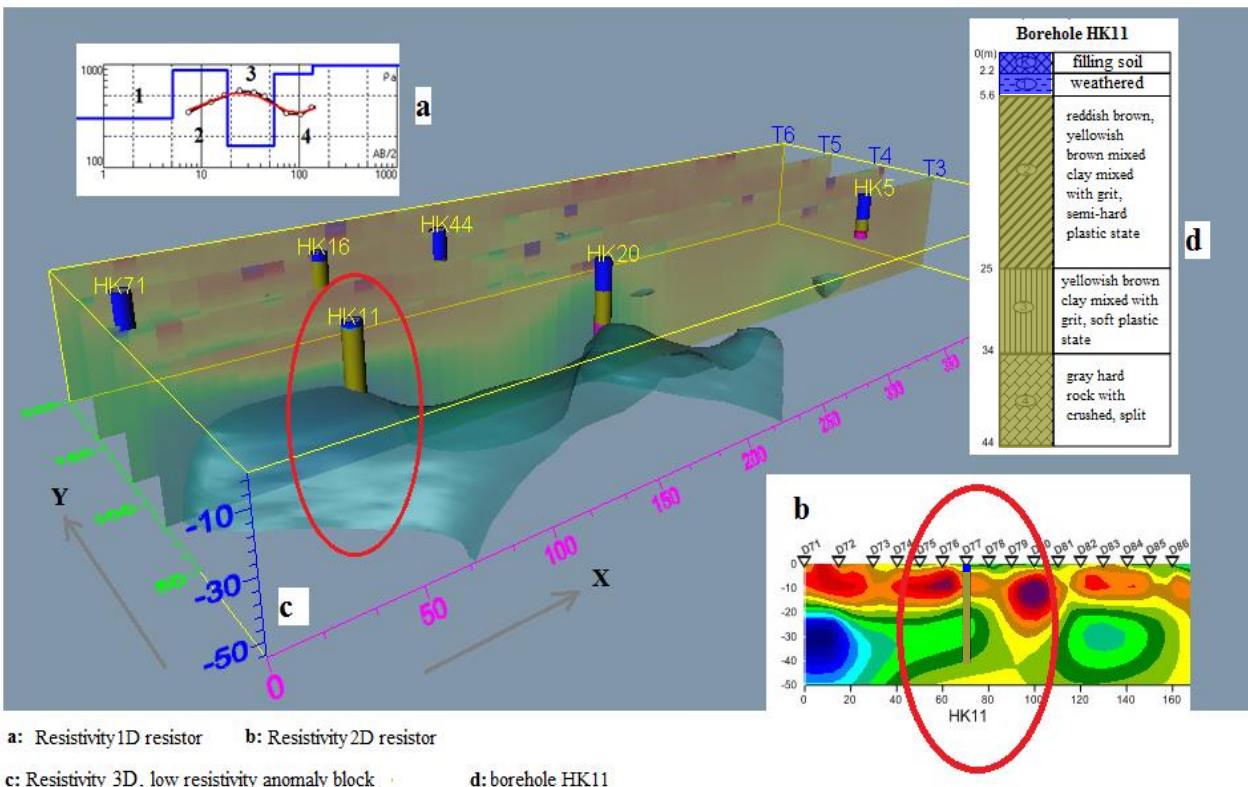


Figure 6. The 3D distribution of the low resistivity anomaly related to fractured zones and caves.



- a: Resistivity 1D resistor
- b: Resistivity 2D resistor
- c: Resistivity 3D, low resistivity anomaly block
- d: borehole HK11

Figure 7. Comparing 1D, 2D, and 3D inversion results with borehole stratigraphy.

The 3D inversion result is slightly different compared to the borehole stratigraphy for the two uppermost soil layers. Because the filling soil is rather thin (2 m) and its resistivity is close to that of the weathered soil. These properties of the filling soil lead to the indistinguishable results of the 3D ERT method due to the spacing of the measuring points. With the lower layers, the 3D inversion results are matched with the borehole information.

5. Conclusion

The 3D inversion results give a clear and detailed spatial distribution of the fractured zones and caves in the study area. The results help to evaluate the volume and position of the interesting object in the subsurface more accurately than that of 1D and 2D investigations.

When we have sufficiently detailed electrical sounding data, the 3D inversion provides the results that are close to the borehole stratigraphy. We propose to use this inversion technique in other regions with dense electrical observation. This technique will help to increase the accuracy and effectiveness of a wide range of interesting studies.

Author contributions

Dat Ngoc Pham - conceptualization, methodology, writing the original draft, formal analysis; Kien Ngoc Pham - formal analysis writing-review & editing; Phong Hop Lai - investigation, survey management, review & editing; Ninh Thi Duong - data curation, software; Trang Hong Pham - geological borehole analysis, review & editing; Tuan Dang Tran - visualization.

References

Bui, T. L. (2012). Research and assessment of geological conditions of works serving the construction of high-rise buildings in Quoc Oai district, Hanoi. Master Dissertation. (in Vietnamese).

Doan, V. T., & Vu, C. M. (2008). Accident of karst subsidence and some research results predict dangerous zoning. *Proceedings of the National Scientific Conference: "Geological catastrophe and prevention solutions"*, Hanoi, 153-162.

Duszyński, F., Jancewicz, K., Kasprzak, M., & Migoń, P. (2017). The role of landslides in downslope transport of caprock-derived boulders in sedimentary tablelands, Stołowe Mts, SW Poland. *Geomorphology*, 295, 84-101.

Le, N. T. (2012). Contribute to determining the cause of erosion on the banks of the Tien River and Saigon River by geophysical surveys near the ground. *Journal of Earth Sciences*, 34(3), 205-216.

Loke, M. H., & Barker, R. D. (1996). Practical techniques for 3D resistivity surveys and data inversion. *Geophysical Prospecting*, 44, 499-523.

Loke, M. H. (2010). *RES2DINV ver. 3.59. Geoelectrical Imaging 2D&3D*. Geotomo software, 148p.

Ogilvy, R., Meldrum, P., Chambers, J., & Williams, G. (2002). The use of 3D electrical resistivity tomography to characterise waste and leachate distribution within a closed landfill, Thriplow, UK. *Journal of Environmental & Engineering Geophysics*, 7(1), 11-18.

Park, S. (1998). Fluid migration in the vadose zone from 3-D inversion of resistivity monitoring data. *Geophysics*, 63(1), 41-51.

Pham, N. D., Lai, H. P., Duong, T. N., & Pham, N. K. (2018). Application of electric exploration method to study soil cracking and sinking in Ky Son district - Hoa Binh province. *Journal of Science and Technology - Thai Nguyen University*, 181(5), 47-53. (in Vietnamese)

Pidlisecky, A., Haber, E., & Knight, R. (2007). RESINVM3D: a 3D resistivity inversion package. *Geophysics*, 72, H1-H10

Represas, P., Santo, F. M., & Mateus, A. (2005). A case study of two and three-dimensional inversion of dipole-dipole data: the Enfermarías Zn-Pb (Ag, Sb, Au) Prospect (Moura, Portugal). *Near Surface Geophysics*, 3(1), 21-31.

Soupios, P. M., Georgakopoulos, P., Papadopoulos, N., Saltas, V., Andreadakis, A., Vallianatos, F., & Makris, J. P. (2007). Use of engineering geophysics to investigate a site for a building foundation. *Journal of Geophysics and*

- Engineering*, 4(1), 94-103.
- Spitzer, K. (1998). The three-dimensional DC sensitivity for surface and subsurface sources. *Geophysical Journal International*, 134, 736-46.
- Sultan, S. A., & Monteiro Santos, F. A. (2008). 1D and 3D resistivity inversions for geotechnical investigation. *Journal of Geophysics and Engineering*, 5(1), 1-11.
- Sultan, S. A., Santos, F. M., & Helal, A. (2006). A study of the groundwater seepage at Hibis Temple using geoelectrical data, Kharga Oasis, Egypt. *Near Surface Geophysics*, 4(6), 347-354.
- Szalai, S., Szokoli, K., Novák, A., Tóth, Á., & Metwaly, M. (2014). Fracture network characterisation of a landslide by electrical resistivity tomography. *Natural hazards and earth system sciences*, 2(6), 3965-4010.
- Weller, A., Frangos, W., & Seichter, M. (2000). Three-dimensional inversion of induced polarization data from simulated waste. *Journal of Applied Geophysics*, 44(2-3), 67-83.
- Yi, M. J., Kim, J. H., Song, Y., Cho, S. J., Chung, S. H. & Suh, J. H. (2001). Three-dimensional imaging of subsurface structures using resistivity data. *Geophysical Prospecting*, 49(4), 483-497.
- Zhang, J., Mackie, R. L., & Madden, T. R. (1995). 3-D resistivity forward modelling and inversion using conjugate gradients. *Geophysics*, 60(5), 1313-1325.
- Zhao, S. K., & Yedlin, M. J. (1996). Some refinements on the finite-difference method for 3-D dc resistivity modeling. *Geophysics*, 61(5), 1301-1307.